International Journal of Innovative Technology and Exploring Engineering (IJITEE)
ISSN: 2278-3075 (Online), Volume-10 Issue-1, November 2020

Corrugated Steel Tunnels – Numerical Study Using Finite Element and Analytical Methods

Ahmed ABDEL-RAHMAN, Mahmoud AWAD-ALLAH, Nashwa SOLIMAN

Abstract*: Corrugated metal pipes, fabricated from galvanized steel, are among the most common structures employed to construct, culverts, underpasses, etc. in the world. Furthermore, the merits of this system over the traditional concrete structures are: lightweight structure, great strength relative to their mass, ease of transport and installation, and low cost. However, application of such construction system in Egypt is not commonly used yet, and many technical problems have been observed during and after construction. Consequently, this paper investigates the deformations around buried steel structures, axial forces and bending moments induced in structures due to back-filling and external loading. Furthermore, two case studies of buried steel projects have been presented in this paper. The first case study has been simulated using finite element method while the second one has been analyzed using analytical methods given in the literature and well-known codes of practice. Thus, an elaborated comparative study has been performed between finite element results and those obtained from analytical methods.

Keywords*: Steel tunnel, finite element method, buried structures, deformations, vertical displacement, soil-structure interaction.

I. INTRODUCTION

Corrugated metal pipes, fabricated from sheets of galvanized steel, are amongst the most common structures employed to construct (Fig. 1): culverts, bridges, underpasses, culvert relining, erosion protection, sheet water drainage, batter and toe drains, and void forms in North America and Europe. Furthermore, the merits of this system over the traditional concrete structures are: lightweight steel structure, great strength relative to their mass, ease of transport and installation, low cost, and durability. However, the application of such construction system in Egypt is not commonly used so far, and many technical problems have been observed during and after construction. Some example of the common problems includes: (1) backfill and its compaction provisions, (2) inappropriate use of the tunnel by people, as a result these problems cause deterioration of the structure with time.

Most of the upcoming national urbanization potential development in Egypt will mandate the construction of tunnels, railways intersections, culverts, underpass, etc. Meanwhile, reducing the construction cost of those infrastructures is the main goal for the decision makers, and using this new technology in construction will deduct the cost of construction by 30-40% less than using traditional reinforced concrete system.

Several researches have been conducted to investigate the performance of the flexible corrugated steel tunnels (CSTs) using either full scale field tests, small scale laboratory tests or finite element modeling, during the different phases of tunnel construction, backfilling and under static and dynamic loading.

Wysokowski and Janusz (2007), and Wysokowski and Howis (20012) carried out laboratory tests to study the effect of backfilling process on steel type tunnels. They found that the main loading on the tunnel structure comes from the backfill material around the tunnel. Therefore, the properties of the backfilling materials should be chosen with certain characteristics. For durability, the zinc anticorrosion protection is appropriate for typical service environmental conditions, while the trench coating is better in case of severe environmental conditions. Esra and Raid (2009) carried out a full-scale static, dynamic and braking tests on a long span corrugated steel culvert. In their work, they found that speed has a significant effect on the dynamic responses of the culvert. Vaslestad et al. (2002) reported field measurements of a corrugated steel culvert constructed as a replacement of corroded concrete bridge in Poznan in Poland. They concluded that the stresses induced and the deformations occurred in the culvert corrugated steel sections during backfilling process are greater than those occurred during live loads case of loading. Furthermore, it was found that for long term response the stresses measured were slightly reduced with time which can be attributed to that the backfill material was consolidated by time leading to an increase of the bearing load on the surrounding media of soil.

Connection strength sometimes is the controller of the soil corrugated steel structure design. Seung and Jong (2007) proposed a new 4-bolt arrangement by increasing the number of rows from two to three rows. Experimental tests on the proposed arrangement proved that this arrangement provides the required compressive seam strength in addition to increasing the flexural performance of the seam.

Revised Manuscript Received on November 30, 2020.
***** Correspondence Author
Ahmed ABDEL-RAHMAN, Professor of Geotechnical Engineering, Department of Civil Engineering, National Research Center, Cairo, Egypt. Email: ahosny66@hotmail.com.
Mahmoud F. AWAD-ALLAH*, Professor Assistant, Researcher, Department of Civil Engineering, National Research Center,Cairo, Egypt (corresponding author Email: mf.awad-alla@nrc.sci.eg).
Nashwa SOLIMAN, Researcher Assistant, PhD candidate, Department of Civil Engineering, National Research Center Cairo, Egypt. Email: nsoliman1985@gmail.com

Corrugated metal pipes

Buried Tunnel

Culvert

Small bridge

Fig. 1.Corrugated metal pipe sections and some of their applications in construction.

Hesham and John (2012) investigated the effect of the corrugated steel plate thickness, bolts arrangement, and initial bolts misalignment on the seam fatigue strength under cyclic loading. Results showed that lap joints affect the fatigue strength of the connection. Correct lap joints with no misalignment are the best with respect to fatigue strength, while incorrect lap joints and initial misalignments result in considerable reduction in the connection fatigue strength.

In addition to the above-mentioned Literature, three of the well-known international codes of practice for design and construction of corrugated metal buried structures have been used in this study, namely: Canadian highway bridge design code (CHBDC, 2007), American Association of State Highway Transportation Officials (AASHTO, 2012), and Design of soil steel composite bridges Sweden manual (Sweden design manual, 2014). Moreover, several field studies on corrugated steel culverts have been reported in the Literature, e.g., Machelski et al (2006), Korusiewicz and Kunecki (2012), and Madaj and Turzbecher (2012). Field measurements and numerical modeling results showed that the steel stress and deformations from live loading were small compared with the steel stress and deformations during backfilling Vaslestad et al (2002), Sidney and David (1988), and Liu et al (2014). Although several approaches have been suggested for design of such structures, no exact theoretical analysis is available yet.

Consequently, this paper investigates the deformation and stress distribution pattern around the buried corrugated metal structures and their long-term behavior as well as the locations of maximum stresses in the tunnel body due to external loads. Moreover, two case studies of buried corrugated steel projects have been introduced in this paper. The first case study has been simulated using finite element method while the second one has been analyzed using analytical methods given in the literature and well-known codes of practice. Thus, a comparative study between vertical and horizontal deformations, axial forces, and bending moments measured in the field against corresponding values obtained from finite element method as well as the analytical methods. Based on the results of this study, recommendations, precautions, and guidelines for construction and design of corrugated metal structures have been introduced.

II. PROCEDURE FOR PAPER SUBMISSION

Two case studies of buried corrugated steel projects have been implemented in this study. The first case study is for a full-scale moving load test which has been modeled using finite element method, and then the proposed finite element model has been calibrated against the field measurements in terms of vertical and lateral deformations.

On the other hand, the second one has been analyzed using analytical methods given in the well-known codes of practice for design of buried steel tunnel as well as it was simulated using the calibrated finite element model.

Consequently, a comparison study has been performed between finite element results and those obtained from analytical methods.

III. FIRST CASE STUDY

The first case study introduced in this paper is a full-scale moving load test on a bridge which was built and given for use as a detour (by-pass) bridge on national road no. 8, nearby the Niemcza village at south-western Poland Machelski et al (2006).

The aim of using this case study is to calibrate the proposed finite element model against the field measurements of vertical and horizontal deformations.

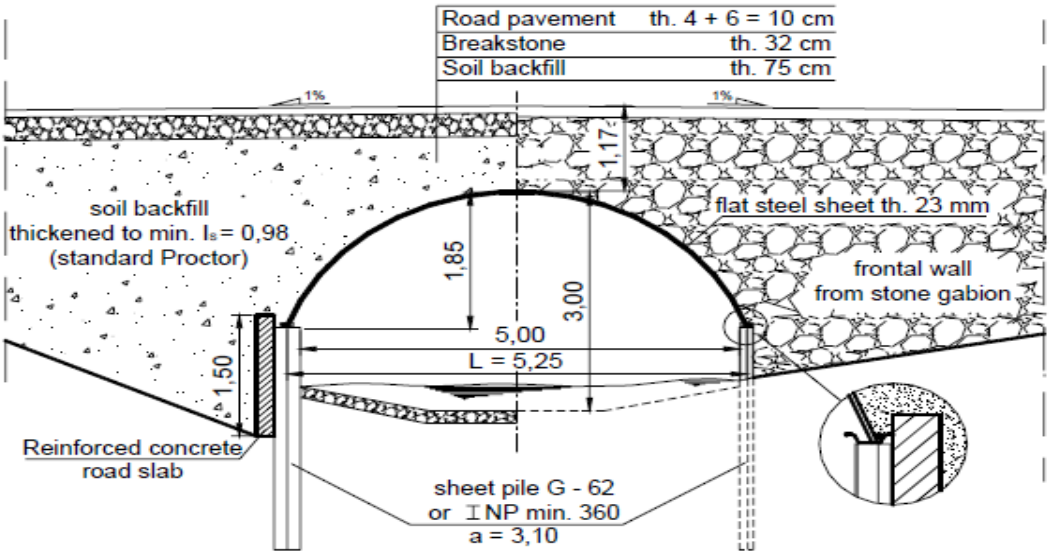

Fig. 2.**Cross section of the first case study used in the finite element analysis (after Machelski et al).**

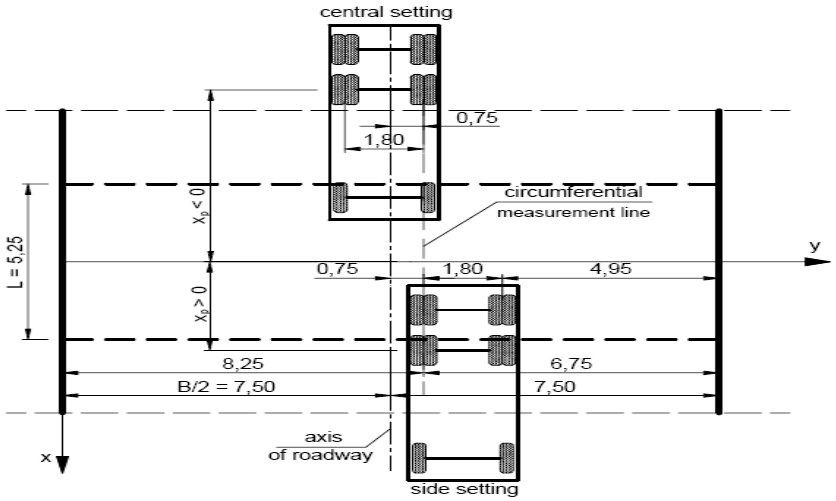

Fig. 3.Vehicle position on the roadway schemes.

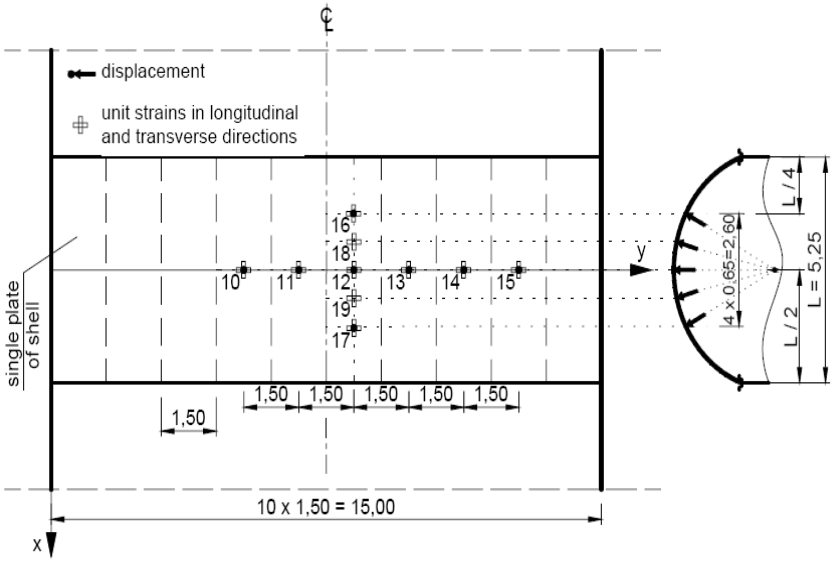

Fig. 4.**Arrangement of the sensors on the bridge plan.**

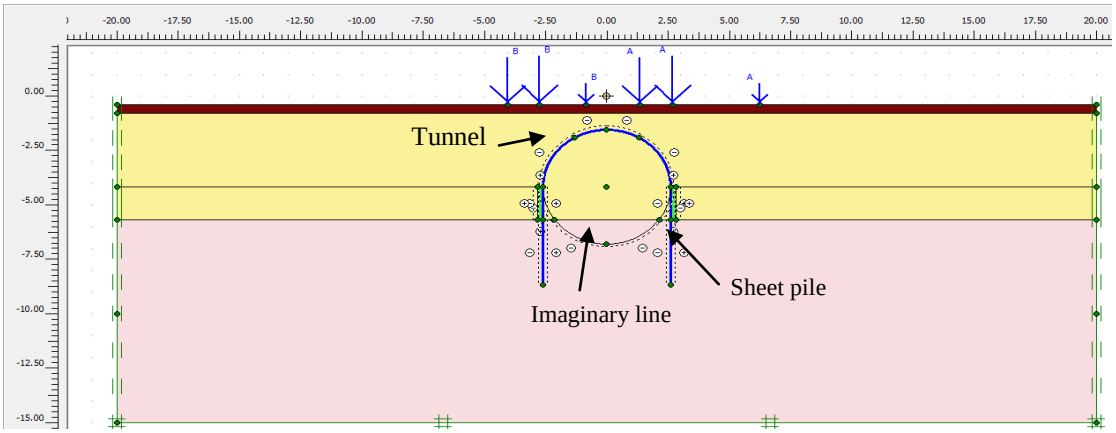

Fig. 5.Geometry, configuration, and moving load arrangement for the proposed FE model.

Fig. 2 shows cross section of the bridge used in the finite element analysis study. The bridge was loaded with the car of TATRA brand of the following weights per axle (according to the order starting with a front axle P1 = 55.6 kN, P2 = 128.3 kN and P3 = 124.6 kN). Fig. 3 illustrates the vehicle position on the roadway bridge schemes. Moreover, during testing the bridge was equipped with sensors and pairs of strain gauges stuck in the circumferential direction and perpendicular to the bottom surface of the steel sheet to measure the stress and deformations during the loading test. The measuring points were set in the circumferential middle line of the shell of a selected steel sheet and on the crown line perpendicular to the roadway bridge axis. Fig. 4 shows the arrangement sensors and strain gauges.

The vehicle position on the length of the bridge was related to its middle axle (P2) and the crown of the shell, which is shown in Fig. 3 and represented by the following equation:

$$X_p = \frac{a_{23}}{2}.i(1)$$

Where: a_{23} = 1.35 m is the rear wheel track of the vehicle. When i = 0 the middle axle (P2) is situated over the crown line. The values of i are positive or negative integer numbers. The position of the vehicle is distinctly given by the Xp-coordinate as the distance of the vehicle's middle axle from the beginning of the coordinate system (of the crown). For example, when X_p = 2.85 m, the force P1 takes a central position over measuring point 12. The force P2 at this moment is over the spot of the shell support.

A. Finite Element Model

Finite element analysis technique (Plaxis 2D, PLAXIS version 2010), has been used for simulation of the problem. Fig. 5 shows the finite element model geometry, configuration, and loading pattern at Roadway bridge. Tables 1 and 2 give the structural and geotechnical properties for the elements and the soil layers of the model, respectively. The following aspects were adopted in finite element modeling:

- Steel sheet of the buried shell was a circumferential strip made from beam elements with three degree of freedom per node.
- Soil media was modeled as 15-node triangle element of a two-dimensional isotropic continuum. Moreover, numerical analyses were carried out by applying constitutive model of Hardening Soil Model (HSM), which describes the elasto-plastic and stress dependent behavior of soil Vermeer and Borst (1984), Stolle (1991), Schanz and Vermeer (1996), Li and Dafalias (2000), Bolton (1986), and Adachi and Oka (1982). On the other hand, the constitutive models applied for road super-structure and weathered rock were linear elastic models.
- Interface reduction factor between the soil materials and steel structures were varied between 0.8 and 0.5 during finite element modelling iterations.

Table- 1: Properties of structural elements.

Structureelement	Young's Modulus (MPa)	Poisson's ratio, ν	Section area mm^2/mm	Moment of inertia mm^4/mm	Yield stress of steel (MPa)
Steel shell	205000	0.3	4.736	1813.8	235
Sheet pile (INP no. 360)	205000	0.3	97	818000	235
Reinforced concrete road slab	21000	0.15	-------	-------	-----

Table-2: Soil parameters used in the FE model (Case study No. 1).

Soil Layer	Material Model	γ kN/m3	c′ kPa	ϕ′ Deg.	Ψ Deg.	Stiffness modulus (MPa)			m	ν	R
						E50	Eoed	Eur			
Road structure	LinearElastic	23	---	---	---	180	---	---	---	0.15	1.0
Backfill	Hardening-Soil	18	0	35	5	60	60	180	0.5	0.3	Variable
Weathered rock	LinearElastic	22	---	---	---	120	---	---	---	0.2	1.0

Note: (γ) = unit weight of soil, (c′)= drained cohesion, (ϕ′)= drained friction angle, (Ψ)= dilatancy angle, (E_{50})= secant stiffness for consolidated drained triaxial test, E_{oed}= tangent oedometer stiffness, E_{ur}= unloading-reloading stiffness, m= power for stress-level dependency of stiffness (ν)= Poisson ratio, and(R)= Interface reduction factor.

B. Construction SequenceSimulation

Modeling of construction sequence of the bridge includes many activities. The sequence of construction includes the following activities:

1- Installation of sheet pile wall, reinforced concrete road slab, backfilling to the top of reinforced concrete road slab.
2- Installation of steel shell and backfilling up to 0.75m to cover the top level of buried steel shell.
3- Execution of the road super-structure.
4- Applying the impact of moving load test (Vehicle of TATRA brand P1 = 55.6 kN, P2 = 128.3 kN and P3 = 124.6 kN).

IV. CALIBRATION OF THE ADOPTED FINITE ELEMENT MODEL

Calibration of the proposed model was conducted with respect to the measured vertical displacement at point 12 (refer to Fig. 4) and the measured horizontal displacement at the spot of the steel sheet support.

A. Simulation of Moving Load Test

To simulate the influence of the moving loads in finite element model solution, the three axles of the vehicle wheels has been located at certain locations based on Eq. 1. The locations of the live loads are calculated at (i= 0, ±1, ±2, ±3, and ±4), which gave X_p-coordinate of P2 (0, ±0.675, ±1.35, ±2.025, and ±2.7), respectively. Fig. 6illustrates the deformed mesh models after loading of live loads on the roadway at i=0 (i.e., the middle axle P2 is situated over the crown line). For every run of the model, both of vertical displacement at point no. 12 and lateral displacement at the steel sheet support were determined in order to be compared versus the field measurements.

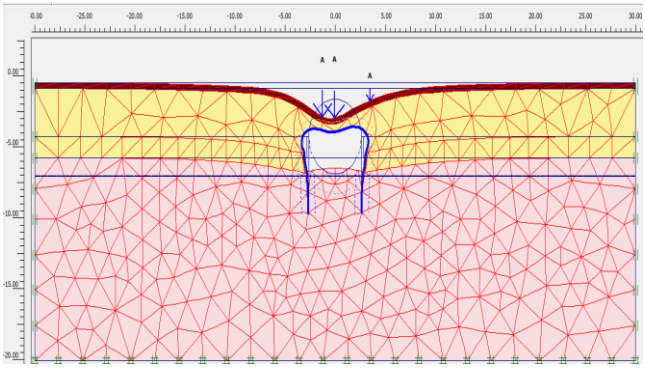

Fig. 6.Deformed mesh due to moving vehicle at i=0 location (i.e., the middle axle P2 is situated over the crown line).

B. Vertical and Lateral Displacement

Fig. 7 depicts the comparison between the measured vertical displacements obtained from the field against the corresponding values resulted from finite element model. It is obvious that the FE model results over estimate the vertical displacement. This may be due to the conservative values given to the soil materials. However, the finite element model results almost gave similar trend relationship for structure response due to moving loads of the truck on the roadway bridge as those obtained from field results.

Regarding to lateral displacement, Fig. 8 illustrates the measured lateral displacements at the steel sheet support measured against the corresponding values resulted from FE model. It can be seen that FE model results over estimate the horizontal displacement although the variation in values is not much high as the vertical displacement ones. The FE model results gave a well agreement relationship in terms of structure response to moving loads with the results obtained from field measurements. Calibration of the finite element model against field measurements indicates that the numerical back-analysis of field full-scale test results showed that the behavior of buried corrugated steel structures under backfilling and external loading can be well reproduced by means of a numerical model using the Hardening Soil Model (HSM). Moreover, for accurate numerical modeling for the interface between soil media and buried steel structures, the interface strength should be taken between 0.6 and 0.5.

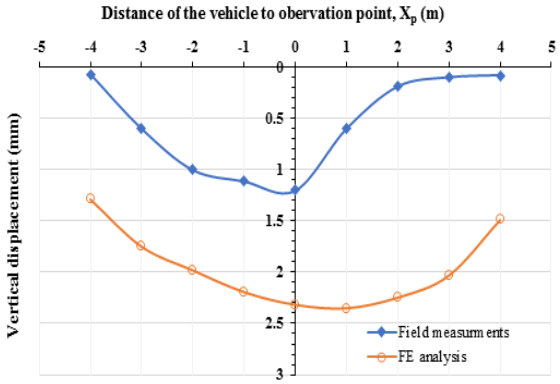

Fig. 7.Comparison between field measured vertical displacements at point 12 against the corresponding values resulted from FE model.

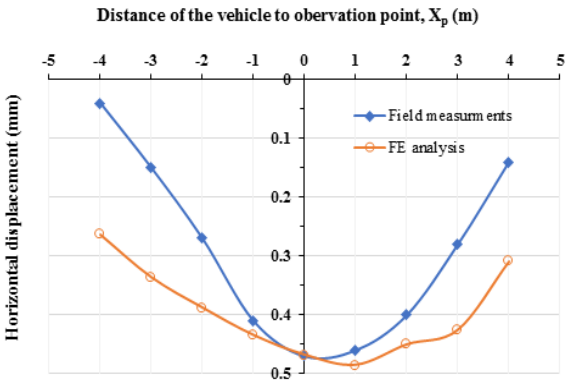

Fig. 8.Comparison between field measured horizontal displacements at steel sheet support against the corresponding values resulted from FE model.

V. SECOND CASE STUDY

The second case study used in this work is a buried corrugated steel structure crossing Rod El-Farag corridor in Cairo, Egypt. This case study has been simulated using the previously calibrated finite element model and designed using the analytical methods. Therefore, a comparison scheme can be carried out between the results of finite element method and analytical method.

Fig. 9 presents geometry of the tunnel profile of span 5.27m and height 4.1m. Corrugated steel section is 200 x 55 mm of thickness 4 mm, and the steel used was hot-dip galvanized in accordance with ISO 1461 (2009). Then, the corrugated steel panels are connected by high strength bolts, where each connection consists of six bolts with 20 mm diameter and ultimate strength F_{ub} = 800 MPa. The steel section properties are given in Table 3.

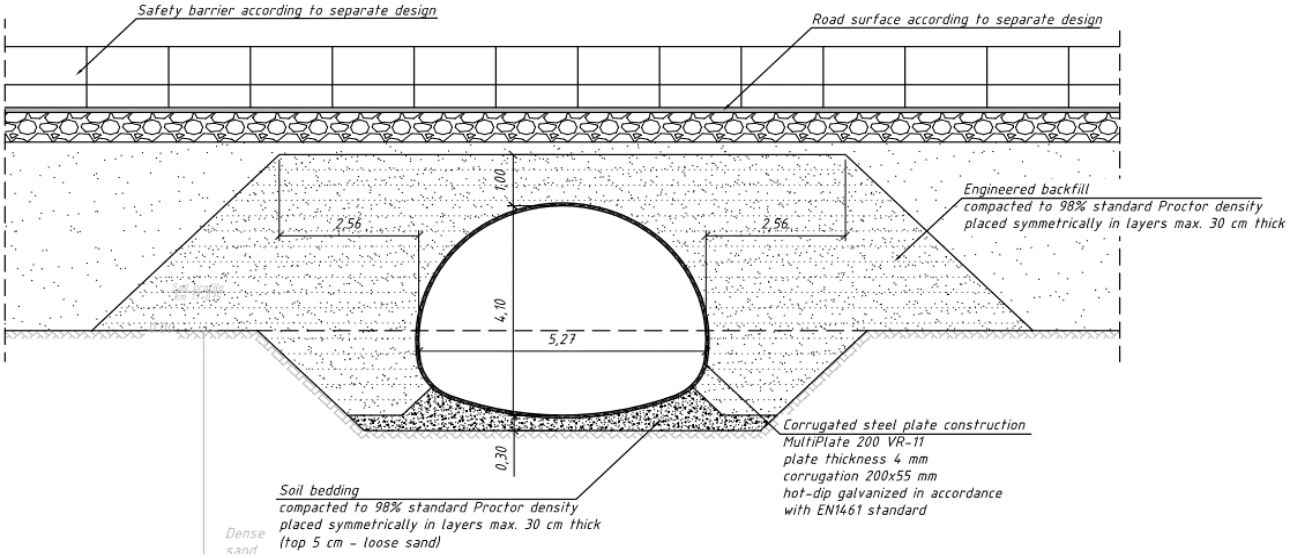

Fig. 9.Cross section of the second case study (all dimension in m).

Table-3: Corrugated steel section properties.

Parameter	Young's Modulus MPa	Poisson's ratio	Section area mm^2/mm	Moment of inertia mm4/mm	Section Modulus mm3/mm	Plastic modulus mm3/mm	Yield stress of steel MPa
Value	200000	0.3	4.736	1813.8	61.49	83.3	235

A. Subsurface Conditions

Field geotechnical investigation of subsurface soil showed that the soil layers encountered in the site can be generally classified as follow: the top strata is natural fill of thickness 0.50m, then it followed by a layer of medium dense to very dense sand of thickness 7.0m, then it followed by very stiff clay of thickness 8.5m, then followed by a thin layer of dense silty sand of thickness 1.5m, then followed by stiff clay layer of thickness 2.0m, and then at the end of borehole a layer of dense sand of thickness 10.5m was found. Ground water level is encountered at a depth of 6.0 m below the ground surface.

B. External Traffic Loads

The imposed loads on the steel tunnel is designed for traffic loads which come from railway and roadway bridges based on Euro code EN 1991-2 (2003). Distribution of external loads in vertical direction is need to be calculated manually because Plaxis is not able to make distribution in Z direction (Plaxis manual, 2010). Assumption is that stresses in soil are distributed in accordance with friction angle of backfill and road super-structure. Fig. 10 shows the load models for roadway and railway loading according to EN 1991-2: 2003. Table 4 gives characteristic values of load for roadway loading adopted by EN 1991-2: 2003. The calculated equivalent applied loads, which was manually input in the finite element model (A-A and B-B) for roadway and railway loading, are presented in Tables 5 and 6, respectively.

Table-4: Characteristic values of load for roadway loading (after EN 1991-2: 2003)

Location	Tandem system	Uniform distribution load system
	Axle loads Qik (kN)	qik or qrk (kN/m2)
Lane number 1	300	9
Lane number 1	200	2.5
Lane number 1	100	2.5
Other lanes	0	2.5
Remaining area (q_{rk})	0	2.5

Note: The details of load model are illustrated in Fig. 13a., Q_{ik}= magnitude of characteristic axle load on notional lane number i (i= 1,2 ….) of a road bridge, q_{ik} = magnitude of characteristic vertical distribution load on notional lane number i (i= 1,2 ….) of a road bridge, q_{rk} = magnitude of characteristic vertical distribution load on the remining area of the carriageway.

Table-5: Calculated equivalent applied loads for roadway bridge

Load pattern in applied FE model	Load based on	Equivalent load
A-A	150 kN+ 100kN	(150+100)/(3.36*0.4)= 186 kPa
B-B	9 kPa	9 kPa

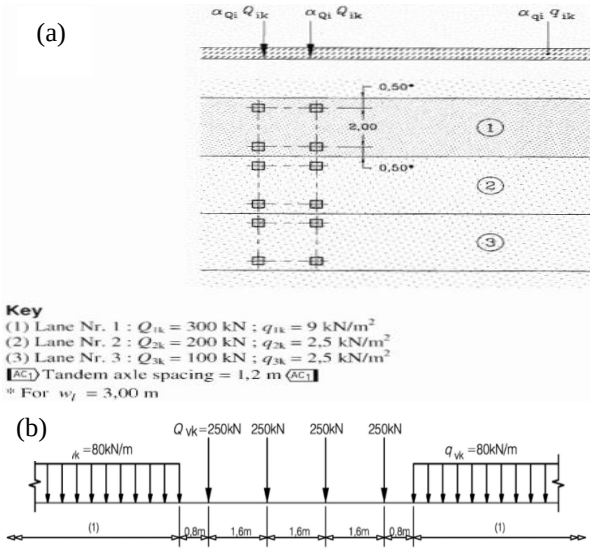

Fig. 10.Load models: (a) for roadway; (b) for railway (after EN 1991-2: 2003).

Table-6:Equivalent applied loads for railway bridge.

Load pattern applied in FE model	Load	Equivalent load
A-A	1.21*4*250/6.4 kN/m	189 kN/n/4.45m = 42.5 kPa
B-B	1.21*80 kN/m	96.8 kN/m/4.45m= 21.8 kPa

C. Analytical Methods for Design of Buried Corrugated Steel Structures

The following three well-known codes of practice for design and construction of steel buried tunnels are used for comparison in terms of normal force and bending moment:

- Canadian Highway Bridge Design Code (CHBDC, 2007)
- American Association of State Highway Transportation Officials (AASHTO, 2012).
- Design of soil steel composite bridges manual (Swedish design manual, 2014).

D. Calculation of Straining Actions Using Analytical Methods

Upon reviewing the set of international design codes implemented in this study, it has become obvious that CHBDC (2007) and AASHTO (2012) consider pure ring compression as their main design criterion.

Therefore, the design output is in the form of thrust force only in the unit of force/unit length along the perimeter of the tunnel section.

On the other hand, Swedish design manual (2014) considers both normal forces and bending moments in the design of the corrugated steel tunnel cross section.

For bending moment, however, CHBDC (2007) considers the bending moments due to construction loads only forchecking of the corrugated steel section capacity, thus it was not considered in the analysis of bending moment esults. Table 7 presents the calculated straining action using the design equations given by the codes of practice.

Table-7: Normal forces and bending moment results obtained from design codes of practice (analytical methods)

Analytical method	Roadway bridge (9 kPa)		Railway bridge (1.21*80 kN/m)	
	Maximum normal force (kN/m)	Maximum bending moment (kN.m/m)	Maximum normal forces (kN/m)	Maximum bending moments (kN.m/m)
CHBDC (2007)	290.7	NA	387.2	NA
AASHTO (2012)	326.2	NA	329.8	NA
Swedish design manual (2014)	349.2	8.8	345	9.21

E. Estimation of Straining Actions Using Finite Element Method

In order to check the corresponding straining actions within the tunnel body finite element model was carried out using PLAXIS 2D version 2010. Table 8 represents the soil parameters used in the FE model. Moreover, FE model configuration, geometry and loading profiles are shown in Figs. 11 and 12 for the roadway and railway bridge locations, respectively.

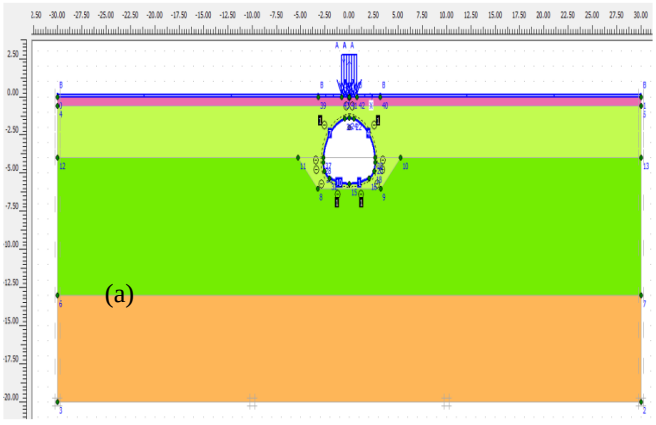

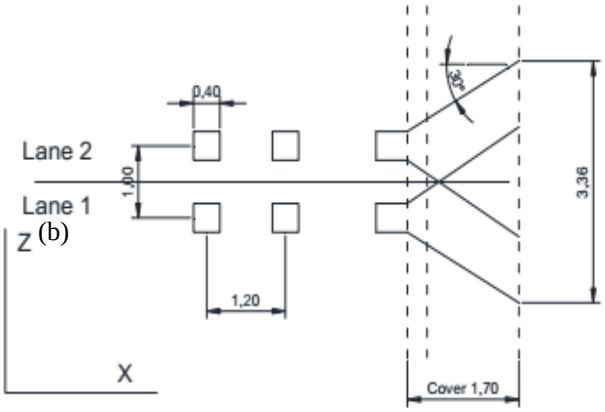

Fig. 11.**Input FEM (a) geometry, configuration, and loading profile for roadway (b) roadway loading distribution in Z-direction (all dimensions in m).**

Table-8: Soil parameters used in the FE model (Case study No. 2)

Soil Layer	Material Model	γ kN/m3	c′ kPa	ϕ′ Deg.	Ψ Deg.	Stiffness modulus MPa			m	ν	R
						E_{50}	E_{oed}	E_{ur}			
Road Structure	Linear Elastic	23	---	---	---	180	---	---	---	0.15	1
Backfill	Hardening-Soil	19	0	32	4	30	30	90	0.5	0.3	Variable
Medium Dense Sand	Hardening-Soil	20	0	34	4	35	35	105	0.5	0.3	1
Hard Clay	Hardening-Soil (Drained)	20	5	25	---	45	45	135	1	0.35	1

Note: (γ) = unit weight of soil, (c′)= drained cohesion, (ϕ′)= drained friction angle, (Ψ)= dilatancy angle, (E_{50})= secant stiffness for consolidated drained triaxial test, E_{oed}=tangent oedometer stiffness, E_{ur}= unloading-reloading stiffness, m= power for stress-level dependency of stiffness(ν)= Poisson ratio, and (R)= Interface reduction factor.

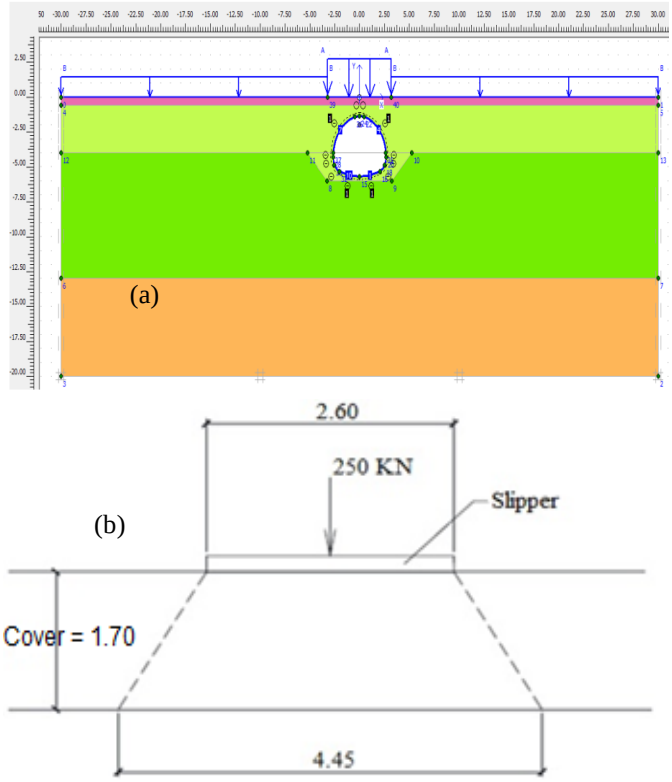

Fig. 12.**Input FEM (a) geometry, configuration, and loading profile for railway (b) railway loading distribution in Z-direction (all dimensions in m).**

Figs. 13, 14, 15, and 6 illustrate the output results of finite element model for railway and roadway locations of the tunnel in terms of vertical displacements, axial forces, and bending moments.

It is obvious that the maximum values of vertical displacement, axial forces, and bending moment of roadway bridge are 7.2cm, 265.8kN/m, and 8.78kN.m/m, respectively. On the other hand, the maximum values of vertical displacement, axial forces, and bending moment of roadway bridge are 5.63cm, 245.37kN/m, and 7.88kN.m/m, respectively.

Furthermore, it is can be noticed that normal forces were found to be almost uniform along the corrugated steel cross section; however, the bending moments have their extreme values at the corners of the corrugated tunnel section. Table 9 gives the summary of the FE results.

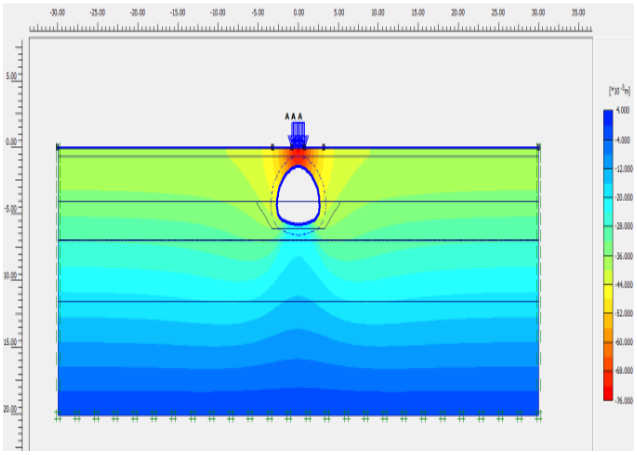

Fig. 13.**Vertical displacement at the roadway location(maximum 7.25 cm).**

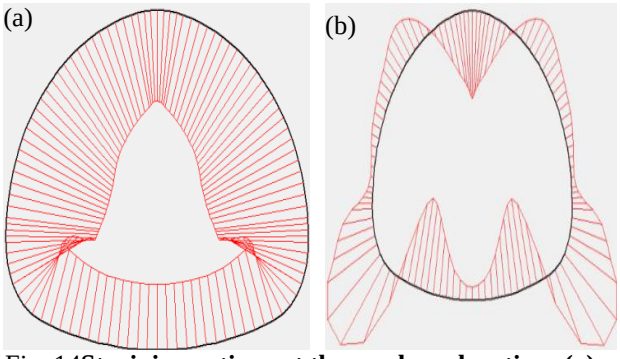

Fig. 14**Straining actions at the roadway location: (a) normal force (extreme = 265.8 kN/m), (b) bending moment(extreme = 8.78 kN.m/m).**

Table-9: Summary of FE model output results

Loading location	Maximum Normal Force (kN/m)	Maximum Bending Moment (kN.m/m)	Maximum Vertical displacement (cm)
Roadway bridge	265.80	8.78	7.25
Railway bridge	243.37	7.88	5.63

Retrieval Number: 100.1/ijitee.A81791110120
DOI: 10.35940/ijitee.A8179.1110120
Journal Website: www.ijitee.org

Published By:
Blue Eyes Intelligence Engineering and Sciences Publication

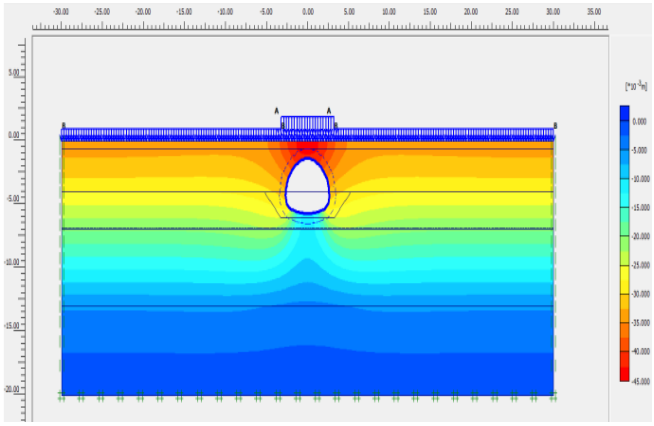

Fig. 15. **Vertical displacement at the railway location (maximum 5.63 cm).**

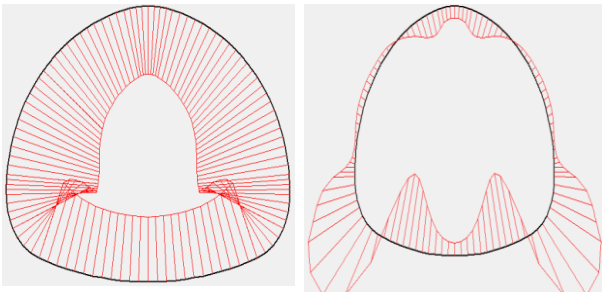

Fig. 16**Straining actions at the railway location: (a) normal force (extreme = 242.37kN/m), (b) bending moment(extreme = 7.88 kN.m/m).**

VI. COMPARITIVE STUDY

In this section an elaborated comparative study has been performed between finite element results and those obtained from analytical methods.Tables 10 and 11 present the results of the analysis of the axial force and bending moment resulted from the loads of roadway and railway bridge using the three different design codes as well as the finite element analysis (Plaxis 2D) results, respectively.

For the calculated axial forces, it is obvious that the three different codes gave values higher than those of finite element results. Comparing to FE results, variations in axial force for roadway and railway loadings are as follows: 9.4 and 59% for CHBDC, respectively; 22.7 and 35.5% for AASHTO, respectively; and 31.4 and 41.7% for Swedish design manual, respectively. Regarding the calculated bending moment values, those values estimated by Swedish design manual were also relatively higher than the values obtained from finite element. The percentages of variations are equal to 0.22 and 16.8% for roadway and railway loadings, respectively.

Table -10: Results of thrust forces form analytical and FE methods.

Loading location	Thrust force (axial forces) (kN/m)			
	CHBDC (2007)	AASHTO (2012)	Swedish design manual (2014)	Finite element analysis
Roadway bridge	290.7	326.2	349.2	265.8
Railway bridge	387.2	329.8	345	243.37

Table- 11 Results of bending form analytical and FE methods.

Loading type	Bending moments (kN.m/m)	
	Swedish design manual (2014)	Finite element analysis
Roadway bridge	8.8	8.78
Railway bridge	9.21	7.88

VII. CONCLUSIONS

In this study, investigation of deformations around buried corrugated steel structures, stresses and bending moments induced in steel structures due to back-filling and loading was performed. Two case studies of buried corrugated steel structured have been implemented in this paper. The first case study has been used for calibration of the proposed finite element model while the second one has been analyzed using analytical methods given in the literature and well-known codes of practice as well as it was simulated using the calibrated finite element model. Thus, a wide comparison study has been performed between finite element results and those obtained from analytical methods. Based on the results of the pervious numerical and analytical studies, the following conclusions can be withdrawn:

- Finite element model has been proposed for simulation of buried steel structures, and it has been calibrated against field measurements obtained from full-scale moving load test. Although the proposed model over-estimates the vertical and lateral displacements, it reveals similar pattern for structure response due to moving loads.
- The numerical back-analysis of field test results showed that the behavior of buried corrugated steel structures under backfilling and external loading can be well reproduced by means of a numerical model using the Hardening Soil Model (HSM). Moreover, for accurate numerical modeling for the interface between soil media and buried steel structures, the interface reduction factor should be taken between 0.6 and 0.5.
- It was observed that normal forces were found to be almost uniform along the corrugated steel cross section; however, the bending moments have their extreme values at the corners of the corrugated tunnel cross section.
- The comparative study indicated that the design equations given in the international codes of practice gave axial forces and bending moments that were greater than those results obtained from finite element method. Therefore, design of such kind of complex structures, which involve soil-structure interaction problem, should be designed using both of finite element and analytical methods to consider all aspects of design.

ACKNOWLEDGEMENT

Authors of this paper gratefully acknowledge the generous financial support from National Research Center of Egypt of the Grand No. 11090335.

REFERENCES

1. Wysokowski, A., Janusz, L. (2007) General conclusions based on the testing of various types of corrugated flexible structures in laboratory in natural scale. Archives of Institute of Civil Engineering, Nr1, 275-286.
2. Wysokowski, A., Howis, J. (2012) Influence of results of testing on manner of constructing culverts and animals passage made as buried flexible steel structures. archives of Institute of Civil Engineering, Nr12, 275-288.
3. Esra, F., Raid, K. (2009) Dynamic testing of a soil steel composite railway bridge. Engineering Structures, 31, 2803-2011.
4. Vaslestad, J., Madaj, A., Leszek, J. (2002) Field Measurements of Long-Span Corrugated Steel Culvert Replacing Corroded Concrete Bridge. Transportation Research Record 1814, Paper No. 02-3415, 164-170.
5. Seung, J., Jong, R. (2007) An experimental verification of the improved bolting arrangement", archives of Institute of Civil Engineering, Nr 1, 109-119.
6. Hesham, M., Kennedy, J.B. (2012) Investigation on fatigue strength of corrugated steel plates bolted lap joints under flexure. archives of Institute of Civil Engineering, 12, 201-213.
7. Canadian Highway Bridge Design Code. 2007.
8. American Association of State Highway Transportation Officials. AASHTO. (2012).
9. Design of soil steel composite bridges Sweden manual. (2014) Volume 2 – Section 2 –Part 6 - BD 12/01- "Design of corrugated steel buried structures with spans greater than 0.9 meters and up to 8.0 meters").
10. Machelski, C., Nntoniszyn, G., Michalski, B. (2006) Live Load Effects on A Soil-Steel Bridge Founded on Elastic Supports. Studia Geotechnica et Mechanica, Vol. XXVIII, No. 2–4, 65-82.
11. Korusiewicz, L., Kunecki, B. (2012) Field Test of a Large-Span Soil-Steel Arch without Stiffeners During Backfilling Operations. Archives of Institute of Civil Engineering, No. 12, 117-123.
12. Madaj, A., Sturzbecher, K. (2012) Changes in Stress Level in A Corrugated Steel Structure Under Long-Term Loads. Archives of Institute of Civil Engineering, No. 12, 159-168.
13. Sidney, H. S., David, k. P. (1988) Modelling soil-structure interaction construction.
    Computers and Structures, 28 (2), 283-288.
14. Liu, B., Liu, Z., Zhang, M., Wang, O. (2014) Study on Impact Parameters of Rigidity and Flexibility for Buried Corrugated Steel Culvert. The Open Civil Engineering Journal, 8, 14-22.
15. Vermeer, P. A., Borst, R. (1984) Non-associated plasticity for soils, concrete, and rock. Heron, 29 (3).
16. Stolle, D.F. (1991) An interpretation of initial stress and strain methods, and numerical stability. International Journal for Numerical and Analytical Methods in Geomechanics, 15, 399-416.
17. Schanz, T., Vermeer, P.A. (1996) Angles of friction and dilatancy of sand. Geotechnique, 46, 145-151.
18. Li, X.S., Dafalias, Y. E. 2000. Dilatancy for cohesionless soils. Geotechnique, 50(4), 145-151.
19. Bolton, M.D. (1986) The strength and dilatancy of sands. Geotechnique, 36(1), 65-78.
20. Adachi, T., Oka, F. (1982) Constitutive equation for normally consolidated clays based on elasto-viscoplasticity. Soils and Foundations, 22, 57-70.
21. ISO 1463 (2009) Metallic and oxide coatings — Measurement of coating thickness — Microscopical method.
22. European Standard, BS EN 1991-2 (2003) Actions on structures - Part 2: Traffic loads on bridges.
23. PLAXIS Manual. (2010) Finite Element Code for Soil and Rock Analysis, 2D Version 2010.1.06380.

AUTHORS PROFILE

Prof. Ahmed Hosny has a substantial experience in a wide range of geotechnical engineering fields. His key skills encompass managing the design and construction of geotechnical-related projects, performing advanced studies and designs, designing and directing geotechnical investigation campaigns, design of foundations of structures on all ground conditions, design and testing of pile foundations, groundwater control, deep braced excavations, etc.

Prof. Hosny participated in carrying out numerical analyses, reviewing designs, editing on specifications, reviewing work submittals, and other major geotechnical- related tasks for many Mega projects carried out in Egypt and abroad for different clients.

Prof. Hosny has a substantial practical and academic experiences in Egypt and many other countries having been involved in various projects and research projects pertaining to soil reinforcement with geosynthetics, numerical modeling of soil/structure interaction using finite elements; and foundation on difficult grounds. Besides publishing more than 36 technical papers and research reports, it is worth noting to the international research collaboration, where he worked as a Principal Investigator on geotechnical and geo-environmental related research projects, that have been jointly funded from the USA National Science Foundation (NSF), and the Egyptian Academy of Science since 1999. The work was carried out through 3 joint research projects with the University of South Florida at Tampa, USA in the field of laboratory and numerical modelling of soil-geogrid interactions under cyclic and monotonic loading, and developing of landfill liners from local materials for the use in landfills.

Dr. Mahmoud F. Awad-Allah has graduated from faculty of Engineering, Kyushu University, Japan. He has more than 15 years of experience in a wide range of geotechnical engineering fields. His major skills encompass managing the design and construction of geotechnical-related projects, performing advanced studies and designs, designing and directing geotechnical investigation campaigns, design of foundations of structures on all ground conditions, design and testing of pile foundations, groundwater control, deep braced excavations, etc. He also has substantial practical and academic experiences in Egypt and many other countries having been involved in various projects, research projects, and academic education for undergraduate students.
Besides, **Dr. Mahmoud Fawzy**is member in many international and national scientific associations such as JSGE, IGSE, and ESGE. He has published more than 20peer-reviewed papers and research reports.

Eng. Nashwa Solimanis Researcher Assistant at the National Research Center of Egypt and PhD candidate in Civil Engineering Department, Faculty of Engineering, Cairo University, Egypt.